SCIENCE CHINA
Chemistry

• ARTICLES •
· SPECIAL ISSUE · Dedicated to the 60th Anniversary of Institute of Chemistry, CAS

October 2016 Vol.59 No.10: 1342–1347
doi: 10.1007/s11426-016-0223-0

N-vinyl pyrrolidone promoted aqueous-phase dehydrogenation of formic acid over PVP-stabilized Ru nanoclusters

Hangyu Liu[1,2], Qingqing Mei[1,2], Yanyan Wang[1,2], Huizhen Liu[1,2*] & Buxing Han[1,2*]

[1]*Beijing National Laboratory for Molecular Sciences, Key Laboratory of Colloid and Interface and Thermodynamics, Institute of Chemistry, Chinese Academy of Sciences, Beijing 100190, China*
[2]*School of Chemistry and Chemical Engineering, University of Chinese Academy of Sciences, Beijing 100049, China*

Received May 13, 2016; accepted July 3, 2016; published online August 30, 2016

In this work, we fabricated the poly(*N*-vinyl-2-pyrrolidone) (PVP)-stabilized ruthenium(0) nanoclusters by reduction of $RuCl_3$ using different reducing agents, and studied their catalytic activity in hydrogen generation from the decomposition of formic acid. It was demonstrated that *N*-vinyl-2-pyrrolidone (NVP), which is a monomer of PVP, could promote the reaction by coordination with Ru nanoparticles. The Ru nanoparticles catalyst reduced by sodium borohydride ($NaBH_4$) exhibited highest catalytic activity for the decomposition of formic acid into H_2 and CO_2. The turnover of numenber (TOF) value could reach 26113 h^{-1} at 80 °C. We believe that the effective catalysts have potential of application in hydrogen storage by formic acid.

carbon dioxide, NVP, ruthenium, dehydrogenation of formic acid

Citation: Liu H, Mei Q, Wang Y, Liu H, Han B. *N*-vinyl pyrrolidone promoted aqueous-phase dehydrogenation of formic acid over PVP-stabilized Ru nanoclusters. *Sci China Chem*, 2016, 59: 1342–1347, doi: 10.1007/s11426-016-0223-0

1 Introduction

Hydrogen, producing only water as a byproduct, has been considered as a promising candidate for the sustainable and clean energy [1]. However, many difficulties still need to be overcome for the practical production, storage, and handling of hydrogen [2]. Various hydrogen storage approaches including metal hydrides [3], sorbent materials [4], and chemical hydride systems [5] are currently being investigated. Among them, formic acid is a renewable bioresource and possible source and reservoir of hydrogen that is safe to use, not flammable, nontoxic, and has a relatively high energy density [6]. Hydrogen can be released via a complete decomposition method, making CO_2 as the only by-product [6–8] (Scheme 1). Furthermore, formic acid can be produced from biomass, so the production of hydrogen from formic acid can be considered as a promising alternative route from the renewable biomass, which has been extensively investigated [9]. However, the undesired reaction pathway (Eq. (2)) should be avoided (Scheme 1) from the perspective of hydrogen storage application [10]. Recently, selective and efficient decomposition of formic acid was achieved with homogeneous organometallic catalysts [11] and heterogeneous noble metals deposited on different supports such as metal oxides and activated carbons [12].

$$HCOOH \longrightarrow CO_2(g) + H_2(g) \quad \Delta G_{298} = -48.8 \text{ kJ mol}^{-1} \quad (1)$$

$$HCOOH \longrightarrow H_2O(l) + CO(g) \quad \Delta G_{298} = -28.5 \text{ kJ mol}^{-1} \quad (2)$$

Scheme 1 Two paths of dehydrogenation of formic acid.

Semi-heterogeneous or Quasi-homogeneous catalysis based on metal nanoparticles (NPs) catalysts combines the virtues of both homogeneous and heterogeneous cataly-

*Corresponding authors (email: liuhz@iccas.ac.cn; hanbx@iccas.ac.cn)

sis. The catalyst can efficiently and selectively catalyze reactions and is easy to be recovered. It exhibits superior catalytic properties in hydrogenation and hydrogenolysis reactions [13–16], such as low-temperature aqueous-phase Fisher-Tropsch synthesis [13], selective hydrogenation of chloronitrobenzene [14], selective hydrogenation of phenol [15] and biphasic aerobic oxidation of alcohols [16]. The superior performances of nanoparticles most likely arise from their controllable sizes and morphologies as well as their unique accessibility to reactants [17,18]. However, the report about the decomposition of formic acid using quasi-homogeneous or semi-heterogeneous catalysis is limited. Tsang and his co-workers [6] reported the decomposition of formic acid over Ag-Pd core-shell nanocatalyst at room temperature; however, the turnover of numenber (TOF) of the catalyst is only 626 h^{-1}.

In this work, we found that *N*-vinyl pyrrolidone (NVP), which is the monomer of poly(*N*-vinyl-2-pyrrolidone) (PVP), could promote the dehydrogenation of formic acid using PVP-stabilized Ru nanocluster as the catalyst. The TOF value was only 1751 h^{-1} in the absence of NVP and could reach 8434 h^{-1} in the presence of NVP. The PVP as the protecting agent and NVP as the ligand synergistically promoted the decomposition of formic acid. The reducing agent $NaBH_4$ could introduce B into the catalyst, and the existence of B also boosted the decomposition of formic acid. After the catalyst was recycled 6 times, the TOF value could reach 26113 h^{-1}.

2 Experimental

2.1 Synthesis of metal NPs

The detailed procedure for synthesizing Ru nanoparticles is similar to that described in the literature [19]. $RuCl_3$ (21 mg, 0.1 mmol) and PVP (111 mg, 1 mmol) were dissolved in 20 mL deionized water in a 100 mL round-bottom flask and stirred for 30 min at 0 °C. A fresh aqueous $NaBH_4$ solution was dropped into the above solution to reduce the Ru^{3+} ions under vigorous stirring. A homogeneous black solution of colloidal dispersion of Ru was obtained after 2 h. The ratio of Ru and $NaBH_4$ was changed from 1:8 to 1:1. The as-prepared catalyst was labelled as Ru-B-PVP-8 and Ru-B-PVP-1. The Ru NPs solution was concentrated to 2 mL and directly used for the dehydrogenation of formic acid. In a similar way, Pt and Pd NPs were synthesized with a molar ratio of metal to PVP 1:10. The as-prepared catalyst was labelled as Pt-B-PVP and Pd-B-PVP.

The Ru nanoparticles using PVA (polyvinyl alcohol) or PEG (polyethylene glycol) as the protecting agent were synthesized using the similar method. The as-prepared catalysts were labelled as Ru-B-PVA and Ru-B-PEG.

The NPs reduced by formic acid were synthesized as follows: $RuCl_3$ (21 mg, 0.1 mmol) and PVP (111 mg, 1 mmol) were dissolved into 2 mL deionized water and 2 mL formic acid in a round bottle under vigorous stirring for 2 h at 353 K. A homogeneous black solution of colloidal dispersion of Ru was obtained. The as-prepared catalyst was labelled as Ru-F-PVP.

2.2 Dehydrogenation of formic acid

In general, a mixture of the as-synthesized catalyst and water (2 mL) was placed in a two-necked round-bottom flask (30 mL), which was placed in an oil bath at 80 °C. A gas burette filled with water was connected to the reaction flask to measure the volume of released gas (temperature kept constant at 298 K during measurements). The reaction started when formic acid (6.5 mmol) and sodium formate (2 mmol) were introduced into the mixture. The molar ratios of Ru/formic acid were theoretically fixed at 0.015 for all the catalytic reactions. The volume of the evolved gas was monitored by recording the displacement of water in the gas burette.

2.3 Durability testing of the catalysts

For testing the durability of catalysts, 6.5 mmol of pure formic acid was subsequently added into the reaction flask after the completion of the first-run decomposition of formic acid and vacuum-rotary evaporation procedure. Such test cycles of the catalyst for the decomposition of formic acid were carried out for 6 runs at 80 °C by adding aliquots of pure formic acid.

2.4 Characterization of metal NPs

X-ray photoelectron spectroscopy (XPS) was performed on the Thermo Scientific ESCALab 250Xi (USA) using 200 W monochromated Al Kα radiation. The 500 μm X-ray spot was used for XPS analysis. The base pressure in the analysis chamber was about 3×10^{-10} mbar. Typically the hydrocarbon C1s line at 284.8 eV from adventitious carbon is used for energy referencing. The transmission electron microscopy (TEM) images of the catalysts were obtained using a TEM JEOL-2011 (JEOL, Japan) with an accelerating voltage of 120 kV. The sample was dispersed in ethanol with the aid of sonication and dropped on an amorphous carbon film supported on a copper grid for the TEM analysis. UV-Vis absorption spectra were recorded with a Persee TU-1901 UV-Vis spectrophotometer (China). The adsorption isotherms of Ru NPs were determined at 298 K in the pressure range of 0–1 atm on a TriStar II 3020 device (Micromeritics Instrument Corporation, USA).

3 Results and discussion

Figure 1 shows the volume of the generated gas (H_2+CO_2)

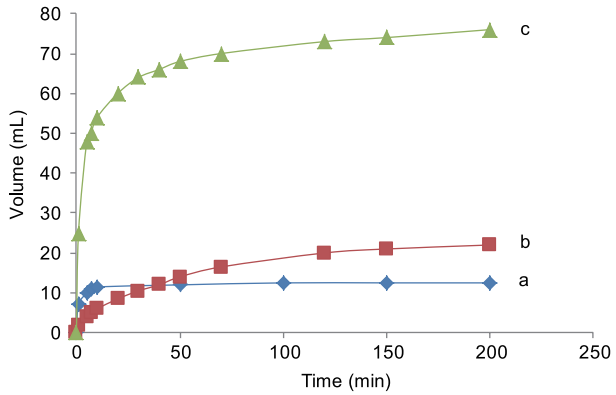

Figure 1 Hydrogen generation from formic acid (6.5 mmol) and sodium formate (2 mmol) over Pt-B-PVP (a), Pd-B-PVP (b) and Ru-B-PVP-8 (c) catalysts. $n_{metal}/n_{formic\ acid}$=0.015, T=80 °C.

versus time for the dehydrogenation of formic acid over Ru-B-PVP-8, Pt-B-PVP and Pd-B-PVP. It shows that Ru-B catalyst exhibited the highest activity for the dehydrogenation of formic acid at 80 °C. The reaction can produce 64 mL gas in 30 min and finally 78 mL (H_2+CO_2) gas could be generated from formic acid at 80 °C over Ru-B-PVP-8 catalyst. The activity of the Pt-B-PVP or Pd-B-PVP was much lower for the reaction and only 12.5 and 22 mL gas could be produced.

The protective agent also has an effect on the activity of the catalyst. The activity of Ru-B-PVP-8, Ru-B-PVA and Ru-B-PEG was compared and the results are shown in Figure 2. The reaction rate of hydrogen gas production at 80 °C in 30 min was determined. The reaction rate of Ru-B-PVA and Ru-B-PEG was much lower than that of Ru-B-PVP-8. The activity of Ru-B-PVA and Ru-B-PEG was similar. The better performance of PVP stabilized Ru nanocluster might be attributed to the existence of nitrogen atom. In the light of the better performance of Ru-B-PVP-8 catalyst, the effect of the other parameters such as reducing agent, the ratio of PVP and Ru was checked. The Ru NPs reduced by formic acid (Ru-F-PVP) yielded much lower reaction rate compared with $NaBH_4$ (Figure 3). The final amount of gas produced was also lower than that of Ru NPs reduced by $NaBH_4$. The reason will be discussed below.

Detailed studies showed that different amount of PVP and $NaBH_4$ also had a significant effect on the reaction rate (Figure 4). By decreasing the ratio of PVP:Ru from 10:1 to 2:1, the reaction rate was decreased. The decrease of the reaction rate might be due to the instability of the catalyst in the presence of less amount of PVP. On the other hand, the conversion of formic acid decreased with decreasing the amount of $NaBH_4$ which might be attributed to that the metal could not be completely reduced.

The reason for the better activity of Ru-B-PVP-8 than that of Ru-B-PVA and Ru-B-PEG may result mainly from the existence of nitrogen atom in PVP. The addition of NVP, which is monomer of PVP, could increase the concentration of nitrogen atom and the reaction rate was greatly improved (Figure 5). Finally, Ru-B-PVP-8 catalyst could release 58%

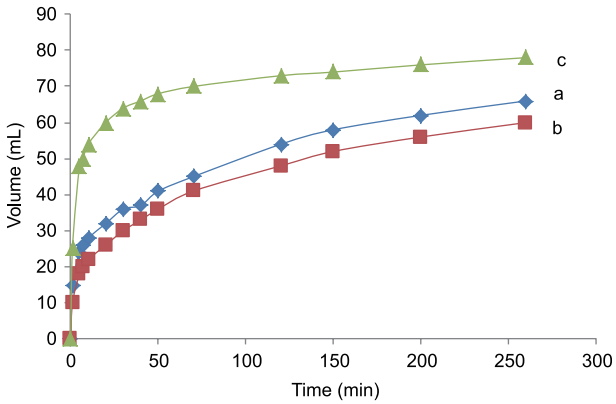

Figure 2 Hydrogen generation from formic acid (6.5 mmol) and sodium formate (2 mmol) over Ru-B-PEG (a), Ru-B-PVA (b) and Ru-B-PVP-8 (c) catalyst. $n_{Ru}/n_{protectant}$=0.1, $n_{Ru}/n_{formic\ acid}$=0.015, T=80 °C.

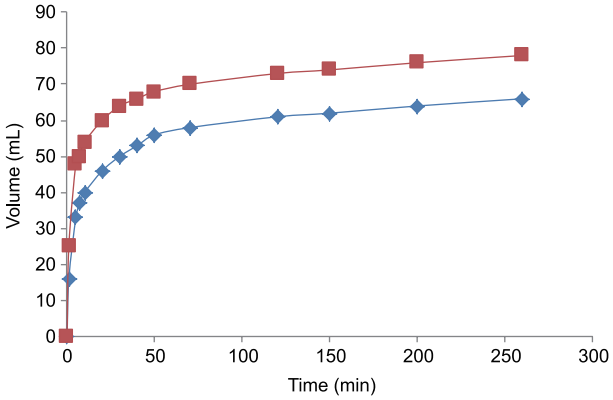

Figure 3 Hydrogen generation from formic acid (6.5 mmol) and sodium formate (2 mmol) over Ru-F-PVP (a) and Ru-B-PVP-8 (b) catalysts. $n_{Ru}/n_{formic\ acid}$=0.015, T=80 °C.

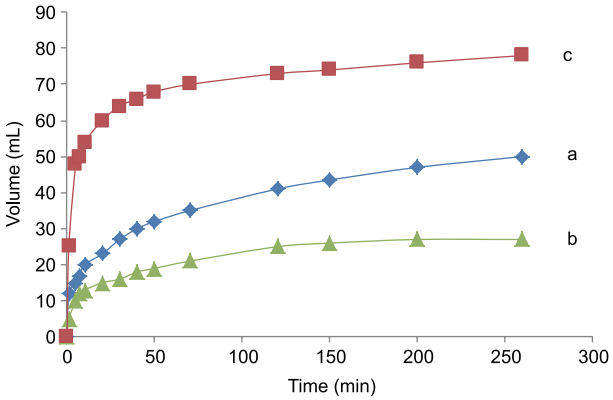

Figure 4 Hydrogen generation from formic acid (6.5 mmol) and sodium formate (2 mmol) over Ru-B-PVP-8 catalysts. (a) PVP/$NaBH_4$/Ru=2:8:1; (b) PVP/$NaBH_4$/Ru=10:1:1; (c) PVP/$NaBH_4$/Ru=10:8:1, $n_{Ru}/n_{formic\ acid}$= 0.015, T=80 °C.

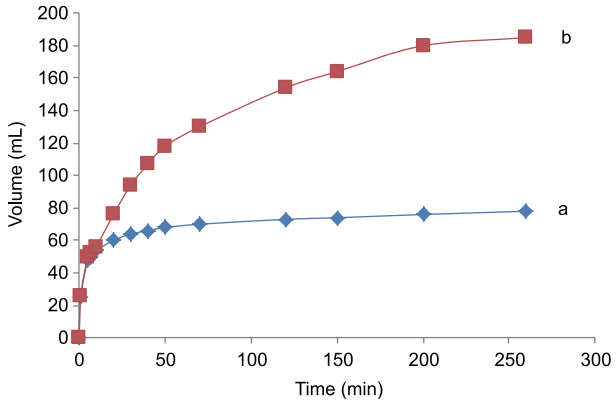

Figure 5 Hydrogen generation from formic acid (6.5 mmol) and sodium formate (2 mmol) over Ru-B-PVP-8 catalysts without (a) and with (b) 2 mL NVP was added. $n_{Ru}/n_{formic\ acid}$=0.015, T=80 °C.

of hydrogen (H_2+CO_2, 185 mL) from formic acid in the presence of NVP, while only 24% of hydrogen (H_2+CO_2, 78 mL) was released in the absence of NVP. The better performance of the catalyst in the presence of NVP may originate from the coordination effect of Ru NPs and nitrogen atom.

Stability and reusability are crucial properties of catalysts. The catalyst Ru-B-PVP-8 in the presence of NVP was reused. It was proved that the catalyst still had excellent catalytic performance after reused 6 times (Figure 6). Interestingly, the activity of the catalyst recycled 6 times was much higher than that of the fresh catalyst, and 330 mL gas (H_2+CO_2) was generated from formic acid at 80 °C, and 99% of formic acid could be decomposed. The surface active metal atoms of the fresh catalyst and the catalyst recycled 6 times were determined by chemisorption method as previously reported [20], and the results are shown in Table 1. The TOF value was calculated based on the surface active metal atoms. The number of surface active metal atoms decreased after recycled 6 times; however, the reaction rate increased. The TOF value could reach 26113 h^{-1} for the catalyst that was recycled 6 times.

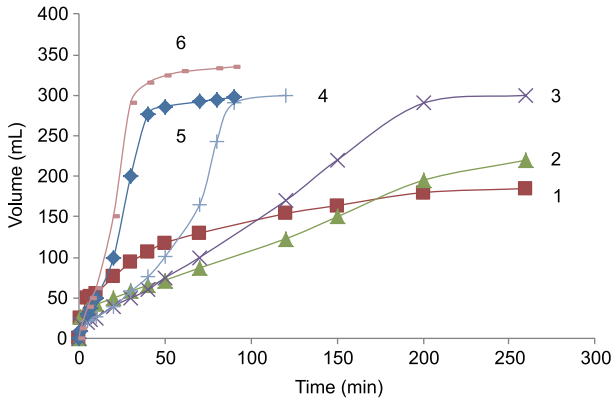

Figure 6 Hydrogen generation from formic acid (6.5 mmol) and sodium formate (2 mmol) recycle 6 times over Ru-B-PVP-8 catalyst. $n_{Ru}/n_{formic\ acid}$= 0.015, NVP 2 mL, T=80 °C.

Table 1 The TOF value of the fresh catalyst and catalyst recycled 6 times [a]

Catalyst	Metal dispersion (%)	TOF (h^{-1}) [b]
Fresh catalyst	0.1305	1751
Recycled catalyst	0.0398	26113

a) Reaction conditions: hydrogen generation from formic acid (6.5 mmol) and sodium formate (2 mmol) over Ru-B-PVP-8 catalyst, $n_{Ru}/n_{formic\ acid}$= 0.015, NVP: 2 mL, T: 80 °C; b) TOF was calculated based on the surface active metal atoms.

To study the reason for the good performance of Ru-B-PVP-8, the catalyst was characterized by UV-Vis method. There was two ultraviolet absorption peaks at 310 and 496 nm for the $RuCl_3$ with PVP. The ultraviolet absorption peaks disappeared for Ru-B-PVP-8 and still existed for Ru-B-PVP-1. It means that 1 equivalent $NaBH_4$ could not completely reduce the Ru(III) and the activity of Ru-B-PVP-1 was lower than that of Ru-B-PVP-8 (Figure 7). The peak at 310 nm moved to 294 nm and the peak at 496 nm disappeared when formic acid was used as reducing agent. Ru(III) could be completely reduced to Ru(0) by $NaBH_4$ for Ru-B-PVP-8, but formic acid could not reduce Ru(III) to Ru(0) at 80 °C for Ru-F-PVP and thus the activity was lower than that of Ru-B-PVP-8. After 6 cycles, there was also no ultraviolet absorption peak. These results indicated that the active component for the decomposition of formic acid was Ru(0).

The morphology and particle size distribution of fresh Ru NPs and that after recycled 6 times was characterized by TEM. Ru nanoparticles with the size around 2.7 nm and narrow size distribution were observed (Figure 8(a)). The morphology and particle size distribution were not changed obviously after reuse (Figure 8(b)). The Ru NPs were characterized by XPS and the results are shown in Figure 9. Ru, B and Cl were detected on the surface of the catalyst for the fresh catalyst, while Cl was not detected for the catalyst after recycled 6 times. It means the Cl was moved from the surface of the catalyst to the bulk phase. This may be one of the reasons

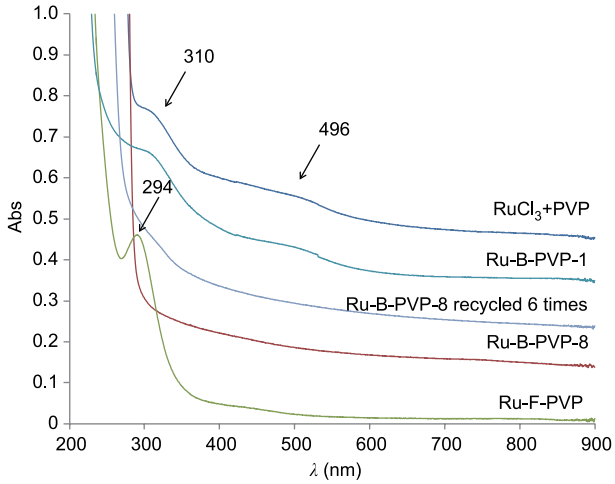

Figure 7 UV-Vis spectra of different catalysts.

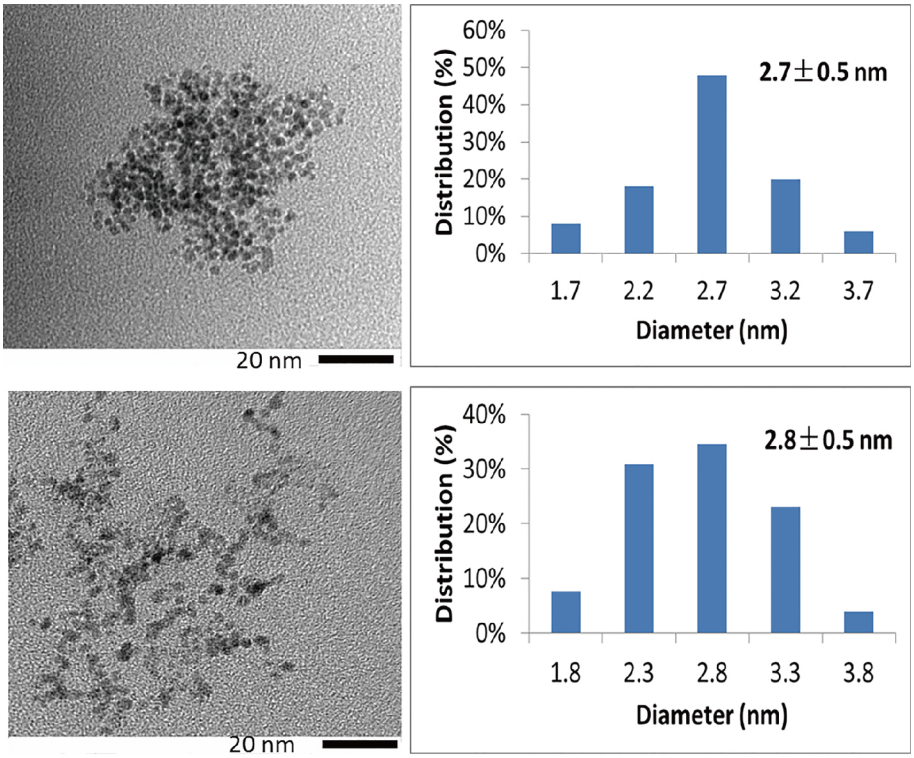

Figure 8 TEM images and particle size distributions of different catalysts. (a) Fresh Ru-B-PVP-8 NPs; (b) Ru-B-PVP-8 NPs after recycled 6 times (color online).

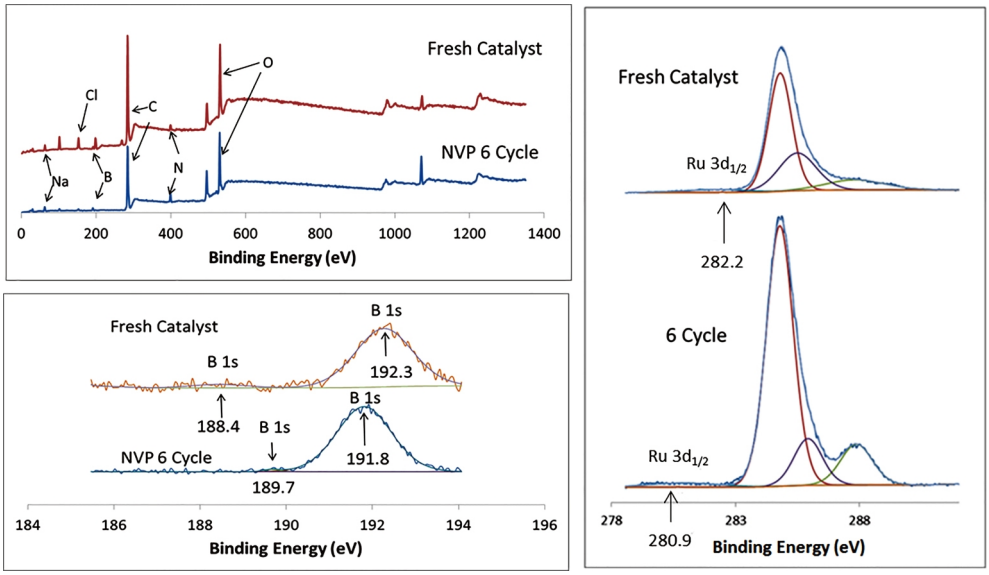

Figure 9 XPS spectra of different catalysts (color online).

for the higher activity of the used catalyst because Cl can poison the catalyst.

The peaks with higher binding energies located at 285.8 and 287.0 eV can be attributed to C–N and C=O structures of PVP, respectively. The peaks at 282.2 and 280.9 eV prove the existence of Ru nanoparticles in the fresh catalyst and recycled catalyst. The peaks at 188.4 and 189.6 eV belong to B(0) and the peaks at 192.3 and 191.8 eV vested in B_2O_3. We can see that the binding energy of Ru, B and B_2O_3 was changed after the catalyst was recycled 6 times. It means that the interaction of Ru and B was changed. This may be another reason for that the activity of the catalyst increased after recycled 6 times. It has been reported that boron-doped Pd nanocatalyst boost the generation of hydrogen from formic acid-for-

mate solutions [21]. That is the reason why the activity of Ru-B-PVP is higher than that of Ru-F-PVP.

4 Conclusions

In summary, the soluble Ru nanoparticles stabilized by PVP are efficient catalyst for the dehydrogenation of formic acid in water. The activity of the catalyst synthesized using $NaBH_4$ as the reducing agent is higher than that of the catalyst reduced by formic acid, and one of the reasons is the existence of B in the catalyst reduced by $NaBH_4$. The active component of this catalyst is Ru(0). The Ru catalysts are more active than the other metal catalysts, including Pt and Pd. The NVP, which is monomer of PVP, promoted the dehydrogenation of formic acid. 26113 h^{-1} of TOF can be achieved after the catalyst was recycled 6 times at 80 °C. The high activities of Ru-B-PVP-8 may result from the coordination effect of NVP with Ru NPs. We believe that the effective catalysts have promising potential of application in hydrogen storage by fomic acid method.

Acknowledgments This work was supported by the Recruitment Program of Global Youth Experts of China, Chinese Academy of Sciences (KJCX2.YW.H30), the National Natural Science Foundation of China (21533011, 21321063). The measurements of TEM and XPS were performed at the Centre for Physicochemical Analysis and Measurements in ICCAS.

Conflict of interest The authors declare that they have no conflict of interest.

1 (a) Leitao EM, Jurca T, Manners I. *Nat Chem*, 2013, 5: 817–829; (b) Dalebrook AF, Gan W, Grasemann M, Moret S, Laurenczy G. *Chem Commun*, 2013, 49: 8735–8751; (c) Yang J, Sudik A, Wolverton C, Siegel DJ. *Chem Soc Rev*, 2010, 39: 656–675; (d) Ma S, Zhou HC. *Chem Commun*, 2010, 46: 44–53
2 (a) Schlapbach L, Züttel A. *Nature*, 2001, 414: 353–358; (b) Chen P, Xiong Z, Luo J, Lin J, Tan KL. *Nature*, 2002, 420: 302–304; (c) Orimo S, Nakamori Y, Eliseo JR, Züttel A, Jensen CM. *Chem Rev*, 2007, 107: 4111–4132
3 Graetz J. *Chem Soc Rev*, 2009, 38: 73–82
4 Suh MP, Park HJ, Prasad TK, Lim DW. *Chem Rev*, 2012, 112: 782–835
5 Staubitz A, Robertson APM, Manners I. *Chem Rev*, 2010, 110: 4079–4124
6 Tedsree K, Li T, Jones S, Chan CWA, Yu KMK, Bagot PAJ, Marquis EA, Smith GDW, Tsang SCE. *Nat Nanotech*, 2011, 6: 302–307
7 (a) Gu X, Lu ZH, Jiang HL, Akita T, Xu Q. *J Am Chem Soc*, 2011, 133: 11822–11825; (b) Bulushev DA, Jia L, Beloshapkin S, Ross JRH. *Chem Commun*, 2012, 48: 4184–4186; (c) Enthaler S, von Langermann J, Schmidt T. *Energy Environ Sci*, 2010, 3: 1207–1217
8 (a) Springer TE, Rockward T, Zawodzinski TA, Gottesfeld S. *J Electrochem Soc*, 2001, 148: A11–A23; (b) Zhu QL, Tsumori N, Xu Q. *Chem Sci*, 2014, 5: 195–199; (c) Qin Y, Wang J, Meng F, Wang L, Zhang X. *Chem Commun*, 2013, 49: 10028–10030
9 (a) Jiang HL, Singh SK, Yan JM, Zhang XB, Xu Q. *ChemSusChem*, 2010, 3: 541–549; (b) Fellay C, Dyson PJ, Laurenczy G. *Angew Chem Int Ed*, 2008, 47: 3966–3968; (c) Ojeda M, Iglesia E. *Angew Chem Int Ed*, 2009, 48: 4800–4803; (d) Loges B, Boddien A, Gärtner F, Junge H, Beller M. *Top Catal*, 2010, 53: 902–914; (e) Boddien A, Mellmann D, Gartner F, Jackstell R, Junge H, Dyson PJ, Laurenczy G, Ludwig R, Beller M. *Science*, 2011, 333: 1733–1736; (f) Hull JF, Himeda Y, Wang WH, Hashiguchi B, Periana R, Szalda DJ, Muckerman JT, Fujita E. *Nat Chem*, 2012, 4: 383–388; (g) Grasemann M, Laurenczy G. *Energy Environ Sci*, 2012, 5: 8171–8181; (h) Martis M, Mori K, Fujiwara K, Ahn WS, Yamashita H. *J Phys Chem C*, 2013, 117: 22805–22810; (i) Moret S, Dyson PJ, Laurenczy G. *Nat Commun*, 2014, 5: 4017
10 (a) Sato S, Morikawa T, Saeki S, Kajino T, Motohiro T. *Angew Chem Int Ed*, 2010, 49: 5101–5105; (b) Sato S, Arai T, Morikawa T, Uemura K, Suzuki TM, Tanaka H, Kajino T. *J Am Chem Soc*, 2011, 133: 15240–15243; (c) Yadav M, Xu Q. *Energy Environ Sci*, 2012, 5: 9698–9725
11 (a) Fukuzumi S, Kobayashi T, Suenobu T. *J Am Chem Soc*, 2010, 132: 1496–1497; (b) Boddien A, Loges B, Gärtner F, Torborg C, Fumino K, Junge H, Ludwig R, Beller M. *J Am Chem Soc*, 2010, 132: 8924–8934; (c) Fukuzumi S, Kobayashi T, Suenobu T. *ChemSusChem*, 2008, 1: 827–834; (d) Loges BÃ, Boddien A, Junge H, Beller M. *Angew Chem Int Ed*, 2008, 47: 3962–3965; (e) Himeda Y. *Green Chem*, 2009, 11: 2018–2022; (f) Sponholz P, Mellmann D, Junge H, Beller M. *ChemSusChem*, 2013, 6: 1172–1176; (g) Gan W, Snelders DJM, Dyson PJ, Laurenczy G. *ChemCatChem*, 2013, 5: 1126–1132; (h) Thevenon A, Frost-Pennington E, Weijia G, Dalebrook AF, Laurenczy G. *ChemCatChem*, 2014, 6: 3146–3152
12 (a) Huang Y, Zhou X, Yin M, Liu C, Xing W. *Chem Mater*, 2010, 22: 5122–5128; (b) Zhou X, Huang Y, Liu C, Liao J, Lu T, Xing W. *ChemSusChem*, 2010, 3: 1379–1382; (c) Zhou X, Huang Y, Xing W, Liu C, Liao J, Lu T. *Chem Commun*, 2008, 48: 3540–3542; (d) Ojeda M, Iglesia E. *Angew Chem*, 2009, 121: 4894–4897; (e) Ting SW, Cheng S, Tsang KY, van der Laak N, Chan KY. *Chem Commun*, 2009, 47: 7333
13 Xiao C, Cai Z, Wang T, Kou Y, Yan N. *Angew Chem Int Ed*, 2008, 47: 746–749
14 Xiao C, Wang H, Mu X, Kou Y. *J Catal*, 2007, 250: 25–32
15 Zhu JF, Tao GH, Liu HY, He L, Sun QH, Liu HC. *Green Chem*, 2014, 16: 2664–2669
16 Hou Z, Theyssen N, Brinkmann A, Leitner W. *Angew Chem Int Ed*, 2005, 117: 1370–1373
17 Zhao D, Wu M, Kou Y, Min E. *Catal Today*, 2002, 74: 157–189
18 Li Z, Zhang J, Mu T, Du J, Liu Z, Han B, Chen J. *Colloid Surfaces A*, 2004, 243: 63–66
19 Yan N, Yuan Y, Dyson PJ. *Chem Commun*, 2011, 47: 2529–2531
20 Umpierre AP, de Jesús E, Dupont J. *ChemCatChem*, 2011, 3: 1413–1418
21 Jiang K, Xu K, Zou S, Cai WB. *J Am Chem Soc*, 2014, 136: 4861–4864